

The color dipole picture of the Drell-Yan process

B.Z. Kopeliovich^{a,d}, J. Raufeisen^b and A.V. Tarasov^{c,d}

^aMax-Planck Institut für Kernphysik, Postfach 103980, 69029 Heidelberg, Germany

^bPhysics Division, Los Alamos National Laboratory, Los Alamos, New Mexico 87545

^cInstitut für Theoretische Physik der Universität, Philosophenweg 19,
69120 Heidelberg, Germany

^dJoint Institute for Nuclear Research, Dubna, 141980 Moscow Region, Russia

Abstract

At high energies, Drell-Yan (DY) dilepton production viewed in the target rest frame should be interpreted as bremsstrahlung and can be expressed in terms of the same color dipole cross section as DIS. We compute DY cross sections on a nucleon target with the realistic parameterization for the dipole cross section saturated at large separations. The results are compared to experimental data and predictions for RHIC are presented. The transverse momentum distribution of the DY process is calculated and energy growth is expected to be steeper at large than at small transverse momenta. We also calculate the DY angular distribution and investigate deviations from the $1 + \cos^2 \theta$ shape.

PACS: 13.85Qk; 13.85.Lg; 13.60.Hb

Keywords: Drell-Yan process; dipole cross section; low x

1 Introduction

The Drell-Yan (DY) process in the kinematical region where the dilepton mass M is small compared to the center of mass energy \sqrt{s} is of similar theoretical interest as deep-inelastic scattering (DIS) at low Bjorken- x . Both processes probe the target at high gluon density where one expects to find new physics. In contrast to DIS, where only the total cross section can be measured, there is a variety of observables which can be measured in the DY process, such as the transverse momentum distribution or the angular distribution of the lepton pair.

The color dipole approach to the DY process suggested by one of the authors [1] (see also [2]) provides a convenient alternative to the well known parton model, in particular, it is especially appropriate to describe nuclear effects [1, 3]. However, the dipole approach was not tested so far for the case of proton-proton collisions. In this paper, we calculate different characteristics of the DY process on a proton target.

Although cross sections are Lorentz invariant, the partonic interpretation of the microscopic process depends on the reference frame. In the target rest frame DY dilepton production should be treated as bremsstrahlung, rather than parton annihilation. The space-time picture of the DY process in the target rest frame is illustrated in fig. 1. A quark (or an antiquark) from the projectile hadron radiates a virtual photon on impact on the target. The radiation can occur before or after the quark scatters off the target. Only the latter case is shown in fig. 1.

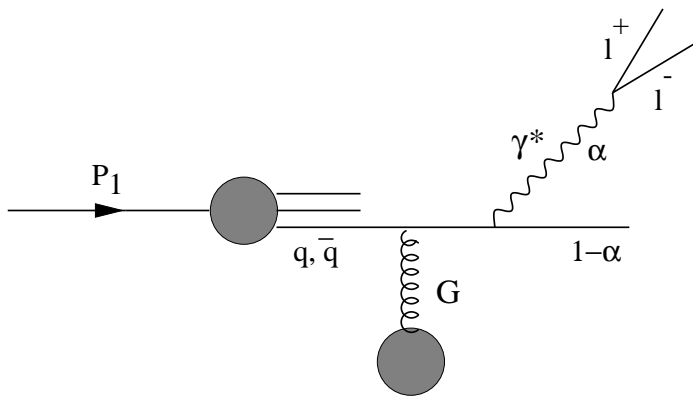


Figure 1: In the target rest frame, DY dilepton production looks like bremsstrahlung. A quark or an antiquark inside the projectile hadron scatters off the target color field and radiates a massive photon, which subsequently decays into the lepton pair. The photon can also be radiated before the quark hits the target.

A salient feature of the rest frame picture of DY dilepton production is that at high energies and in impact parameter space the DY cross section can be formulated in terms of the same dipole cross section as low- x_{Bj} DIS. Note that also the transverse momentum distribution of DY dileptons can be expressed in terms of this dipole cross section [3]. The crucial input to all calculations is the dipole cross section of interaction of a $q\bar{q}$ pair with a nucleon which at present cannot be reliably calculated. We employ the parameterization of Golec-Biernat and Wüsthoff [4], since it describes well all DIS data in the range of Q^2 which is relevant for DY.

As a result of the experimental situation, most work in low- x physics is done for the case of DIS where the structure function F_2 has been measured extensively at

HERA. In contrast to this, only very few data are available on the low- x_2 DY process. This will however change with the advent of RHIC. In this paper, we perform the first comparison between calculations in the dipole picture of DY and the available data. In section 2 we give a description of the color dipole formulation of the DY process. The results of the calculations for DY are presented in section 3.

2 The DY-process in impact parameter space

The cross section for radiation of a virtual photon from a quark after scattering on a proton, can be written in factorized light-cone form [1, 2, 3],

$$\frac{d\sigma(qp \rightarrow \gamma^* X)}{d \ln \alpha} = \int d^2 \rho |\Psi_{\gamma^* q}^{T,L}(\alpha, \rho)|^2 \sigma_{q\bar{q}}(x_2, \alpha \rho), \quad (1)$$

similar to the case of DIS. Here, $\sigma_{q\bar{q}}$ is the cross section for scattering a $q\bar{q}$ -dipole off a proton which depends on the $q\bar{q}$ separation $\alpha\rho$, where ρ is the photon-quark transverse separation and α is the fraction of the light-cone momentum of the initial quark taken away by the photon. We use the standard notation for the kinematical variables, $x_2 = (\sqrt{x_F^2 + 4\tau} - x_F)/2$, $\tau = M^2/s = x_1 x_2$, where x_F is the Feynman variable, s is the center of mass energy squared of the colliding protons and M is the dilepton mass. In (1) T stands for transverse and L for longitudinal photons.

An interesting feature of our approach is the appearance of the dipole cross section in (1), although there is no physical $q\bar{q}$ -dipole in fig. 1. The physical interpretation of (1) is similar to the DIS case. The projectile quark is expanded in the interaction eigenstates. We keep only the first eigenstate,

$$|q\rangle = \sqrt{Z_2} |q_{bare}\rangle + \Psi_{\gamma^* q}^{T,L} |q\gamma^*\rangle + \dots, \quad (2)$$

where Z_2 is the wavefunction renormalization constant for fermions. In order to produce a new state the interaction must resolve between the two Fock states, *i.e.* they have to interact differently. Since only the bare quarks interact in both Fock components the difference arises from their relative displacement in transverse plane. If ρ is the transverse separation between the quark and the photon, the γ^*q fluctuation has a center of gravity in the transverse plane which coincides with the impact parameter of the parent quark. The transverse separation between the photon and the center of gravity is $(1 - \alpha)\rho$ and the distance between the quark and the center of gravity is correspondingly $\alpha\rho$. A displacement in coordinate space corresponds to a phase factor in momentum space. The two graphs for bremsstrahlung, where the photon is radiated either before or after impact on the target, have the relative phase factor $-\exp(i\alpha\vec{\rho} \cdot \vec{k}_\perp)$, which produces the color screening factor $[1 - \exp(i\alpha\vec{\rho} \cdot \vec{k}_\perp)]$ in the dipole cross section.

In Born approximation (two gluon exchange) the dipole cross section is independent of energy. The energy dependence is generated by additional radiation of gluons, which can be resummed in leading $\ln(1/x)$ approximation. With help of the Weizsäcker-Williams approximation and at small separations, the dipole cross section

can be expressed in terms of the unintegrated target gluon density,

$$\sigma_{q\bar{q}}(x_2, \rho) = \frac{4\pi}{3} \alpha_s \rho^2 \int \frac{d^2 k_\perp}{k_\perp^2} \frac{[1 - \exp(i\vec{k}_\perp \cdot \vec{\rho})]}{k_\perp^2 \rho^2} \frac{\partial G(x_2, k_\perp^2)}{\partial \ln(k_\perp^2)}, \quad (3)$$

where k_\perp is the transverse momentum exchanged with the target. This is explained in some detail in [5]. Note that the color screening factor in (3) makes the dipole cross section vanish like $\propto \rho^2$ at $\rho \rightarrow 0$. This salient property of the dipole cross section is the heart of the color transparency phenomenon [6, 7, 8].

In terms of Regge phenomenology, the color dipole approach accounts only for the pomeron part of the cross section, since the dipole cross section (3) is governed by gluonic exchange mechanisms. Therefore, this approach can be applied only at high energies, i.e. at small x_2 . As already mentioned above, the partonic interpretation of scattering processes depend on the reference frame. In terms of the parton model, which is formulated in the infinite momentum frame of the proton, the dipole approach corresponds to annihilation of projectile quarks (antiquarks) with sea antiquarks (quarks) of the target generated via gluons. Note that the statement, whether a sea quark belongs to the target or to the projectile, is frame dependent. If the projectile quark or antiquark becomes slow in the limit $\alpha \rightarrow 1$, it can be interpreted in the infinite momentum frame of the target as anti-seaquark or seaquark of the target which annihilates with the projectile parton. No annihilation with valence quarks from the target is taken into account in the dipole picture. Note also that valence as well as sea parton distributions of the projectile are contained in the parameterization of the projectile structure function in (7). Therefore, the formulation of the DY process presented in this section is not fully symmetric between projectile and target.

In addition to sea quarks generated from gluon splitting there is a part of the sea generated nonperturbatively from the meson cloud of the nucleon [9]. This contribution has received much attention in connection with the \bar{d}/\bar{u} asymmetry measured recently by FNAL E866/NuSea [10]. Since such a sea component steeply decreases at small x_2 , the dipole approach eq. (1) can be safely applied in this region.

The transverse momentum distribution of DY pairs can also be expressed in terms of the dipole cross section [3]. The differential cross section is given by the Fourier integral

$$\begin{aligned} \frac{d\sigma(qp \rightarrow \gamma^* X)}{d \ln \alpha d^2 q_\perp} &= \frac{1}{(2\pi)^2} \int d^2 \rho_1 d^2 \rho_2 \exp[i\vec{q}_\perp \cdot (\vec{\rho}_1 - \vec{\rho}_2)] \Psi_{\gamma^* q}^*(\alpha, \vec{\rho}_1) \Psi_{\gamma^* q}(\alpha, \vec{\rho}_2) \\ &\times \frac{1}{2} \{ \sigma_{q\bar{q}}(x_2, \alpha \rho_1) + \sigma_{q\bar{q}}(x_2, \alpha \rho_2) - \sigma_{q\bar{q}}(x_2, \alpha(\vec{\rho}_1 - \vec{\rho}_2)) \}. \end{aligned} \quad (4)$$

after integrating this expression over the transverse momentum q_\perp of the photon, one obviously recovers (1). The expressions for the LC wavefunctions needed here are

$$\begin{aligned} \Psi_{\gamma^* q}^{*T}(\alpha, \vec{\rho}_1) \Psi_{\gamma^* q}^T(\alpha, \vec{\rho}_2) &= \frac{\alpha_{em}}{2\pi^2} \left\{ m_f^2 \alpha^4 K_0(\eta \rho_1) K_0(\eta \rho_2) \right. \\ &\quad \left. + [1 + (1 - \alpha)^2] \eta^2 \frac{\vec{\rho}_1 \cdot \vec{\rho}_2}{\rho_1 \rho_2} K_1(\eta \rho_1) K_1(\eta \rho_2) \right\}, \end{aligned} \quad (5)$$

$$\Psi_{\gamma^* q}^{*L}(\alpha, \vec{\rho}_1) \Psi_{\gamma^* q}^L(\alpha, \vec{\rho}_2) = \frac{\alpha_{em}}{\pi^2} M^2 (1 - \alpha)^2 K_0(\eta \rho_1) K_0(\eta \rho_2), \quad (6)$$

with $\eta^2 = (1 - \alpha)M^2 - \alpha^2 m_f^2$. We introduce a quark mass $m_f = 200$ MeV. The quark mass has virtually no influence on the numerical results in pp collisions, fig. 2, but will be more important in proton-nucleus collisions [11]. Three of the four integrations in (4) can be performed analytically for arbitrary $\sigma_{q\bar{q}}$ [12].

For embedding the partonic cross section (1) into the hadronic environment, one has to note that the photon carries away the momentum fraction x_1 from the projectile hadron. The hadronic cross section reads then

$$\begin{aligned} \frac{d\sigma}{dM^2 dx_F} &= \frac{\alpha_{em}}{3\pi M^2} \frac{x_1}{x_1 + x_2} \int_{x_1}^1 \frac{d\alpha}{\alpha^2} \sum_f Z_f^2 \left\{ q_f \left(\frac{x_1}{\alpha} \right) + q_{\bar{f}} \left(\frac{x_1}{\alpha} \right) \right\} \frac{d\sigma(qp \rightarrow \gamma^* X)}{d \ln \alpha} \\ &= \frac{\alpha_{em}}{3\pi M^2} \frac{1}{x_1 + x_2} \int_{x_1}^1 \frac{d\alpha}{\alpha} F_2^p \left(\frac{x_1}{\alpha} \right) \frac{d\sigma(qp \rightarrow \gamma^* X)}{d \ln \alpha}, \end{aligned} \quad (7)$$

and similar for the transverse momentum distribution (4). The factor $\alpha_{em}/(3\pi M^2)$ accounts for the decay of the photon into the lepton pair. Remarkably, the parton densities $q_f, q_{\bar{f}}$ of the projectile enters just in the combination F_2^p , which is the structure function of the proton. Therefore we did not include the fractional quark charge Z_f in the DY wavefunctions (5, 6). The structure function F_2^p is needed at large values of x_{Bj} . We employ the parameterization from [13] in our calculations.

The dipole cross section is largely unknown, only at small distances ρ it can be expressed in terms of the gluon density. However, several parameterizations exist in the literature, describing the whole function $\sigma_{q\bar{q}}(x, \rho)$, without explicitly taking into account the QCD evolution of the gluon density. A very economical parameterization is provided by the saturation model of Golec-Biernat and Wüsthoff [4],

$$\sigma_{q\bar{q}}(x, \rho) = \sigma_0 \left[1 - \exp \left(- \frac{\rho^2 Q_0^2}{4(x/x_0)^\lambda} \right) \right], \quad (8)$$

where $Q_0 = 1$ GeV and the three fitted parameters are $\sigma_0 = 23.03$ mb, $x_0 = 0.0003$, and $\lambda = 0.288$. This dipole cross section vanishes $\propto \rho^2$ at small distances, as implied by color transparency and levels off exponentially at large separations, which reminds one of eikonalization. The authors of [4] are able to fit all available HERA data with a quite low χ^2 and can furthermore also describe diffractive HERA data. Although the parameterization (8) might be unrealistic at very large distances (see discussion in [14]), we can safely use it, because DY data are all taken at quite large virtualities, where (8) works well.

3 Calculation of DY cross sections

We can now proceed and investigate how well DY data are reproduced in the color dipole approach. At present, there are however not many data for DY cross sections at low x_2 . We compare to those data for p^2H scattering from E772 [15] which correspond to the lowest values of x_2 . Since the dipole approach is valid at small x_2 , we only compare to points with $x_2 < 0.1$. The result of our calculation, using (7), is shown in fig. 2. The curves for RHIC (dashed curves) correspond of course to lower values

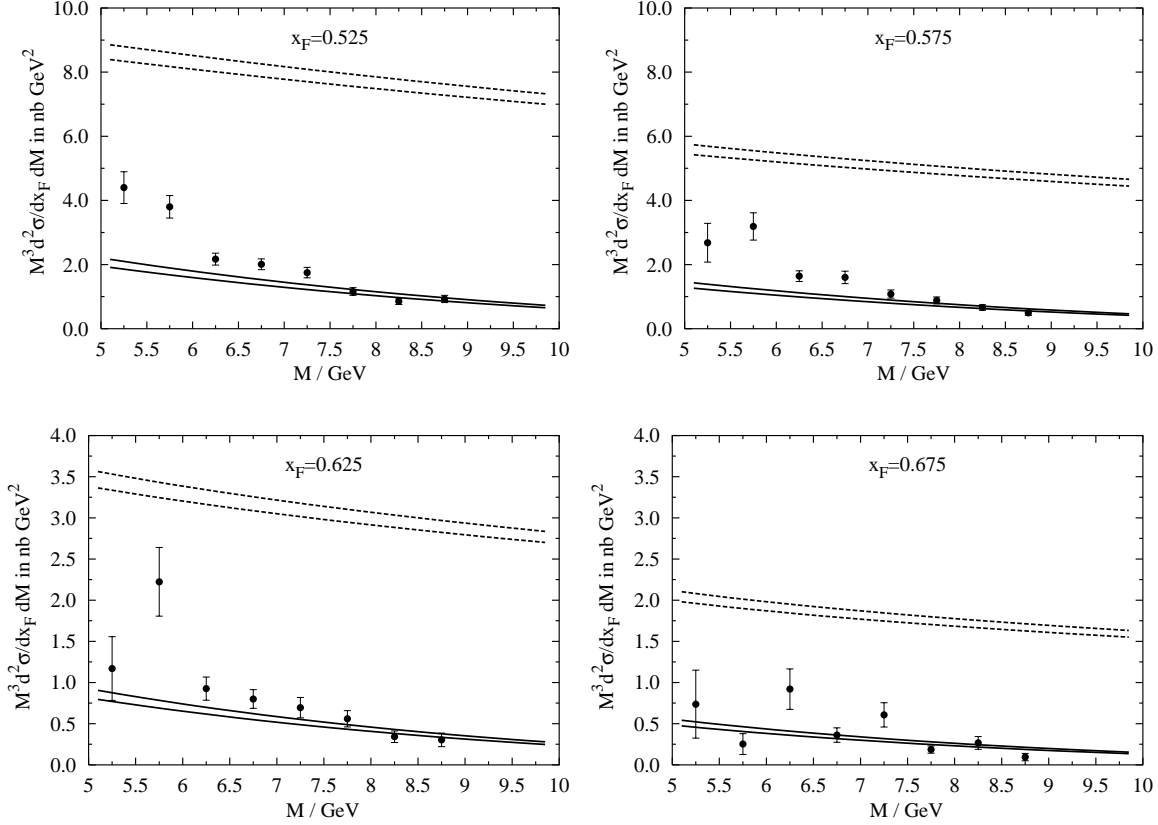


Figure 2: The points represent the measured DY cross section in p^2H scattering from [15]. Only statistical errors are shown. Note that for these points $0.03 \leq x_2 \leq 0.09$. These values of x_2 are already quite large for the dipole approach. The curves are calculated with the dipole cross section (8) without any further fitting procedure. The solid curves are calculated at the same kinematics as the data point (center of mass energy $\sqrt{s} = 38.8$ GeV). The dashed curves are calculated for RHIC energies, $\sqrt{s} = 500$ GeV. For each energy, the lower curve is for quark mass $m_f = 200$ MeV, the upper curve for $m_f = 0$.

for x_2 than the ones for E772. The DY cross section increases, because the dipole cross section increases with energy. No further fitting procedure of the parameters in the dipole cross section (8) was performed. The data, and in particular the absolute magnitude of the cross section is quite well reproduced, except for few points at low mass. We emphasize that the curves in fig. 2 are results of a parameter free calculation. Varying the quark mass m_f leaves the numerical results almost unaffected. Note also that no K -factor was introduced. As pointed out above, in pQCD the dipole approach corresponds to a resummation of logarithms $\ln(1/x)$. However, we do not perform a pQCD calculation, but employ the phenomenological parametrization (8) which is fitted to DIS data. We assume that this parametrization contains also contributions beyond the leading-log approximation, as well as nonperturbative effects. Therefore, we believe that it is not legitimate to use a K -factor in our approach.

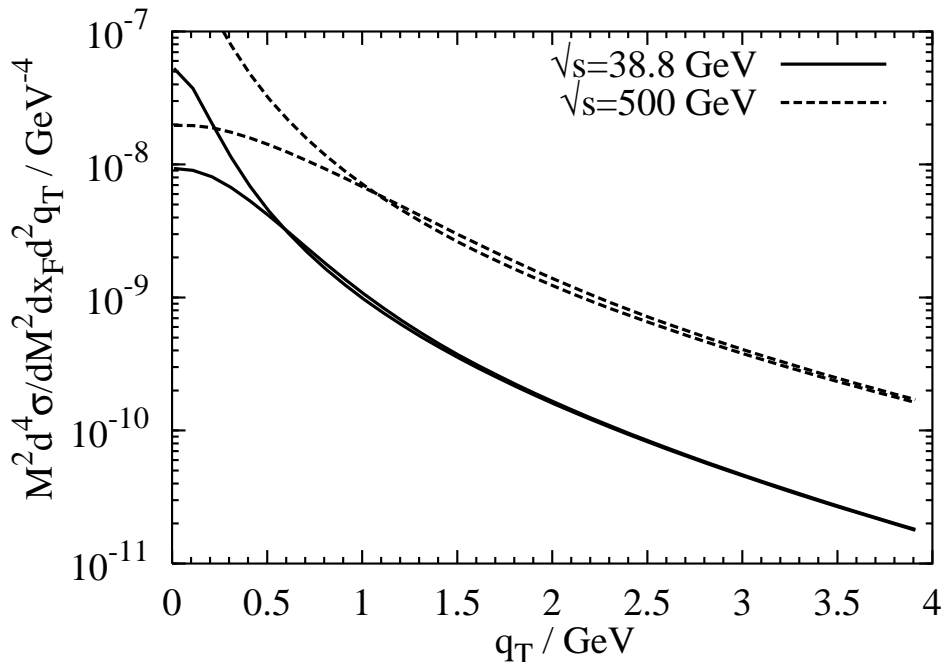


Figure 3: The transverse momentum distribution for DY pairs calculated from (4) at $x_F = 0.625$ and $M = 6.5$ GeV. The curves which flatten at small q_\perp are calculated with the realistic dipole cross section (8), while the other two curves are calculated with the small ρ approximation (9).

Furthermore, we also calculate the transverse momentum distribution of DY dilepton pairs from (4). The result is depicted in fig. 3. The DY cross section is finite at $q_\perp = 0$, in contrast to the first order pQCD correction to the parton model. In the parton model, one has to resum large logarithms $\log(q_\perp/M)$ from soft gluon radiation in order to avoid the divergence at $q_\perp = 0$. In the dipole approach, the cross section does not diverge, because of the saturation of the dipole cross section. In order to find out, how sensitive the transverse momentum distribution to the large ρ -behavior of $\sigma_{q\bar{q}}$ is, we do the same calculation with the small ρ approximation of (8),

$$\tilde{\sigma}_{q\bar{q}}(x, \rho) = \sigma_0 \frac{Q_0^2}{4(x/x_0)^\lambda} \rho^2. \quad (9)$$

The result is shown by the dotted curves in fig. 3. There is no divergence at $q_\perp = 0$, because of the quark mass $m_f = 200$ MeV, but the cross section at small q_\perp is quite strongly affected.

We do not compare to data in fig. 3, because all available data are integrated over x_F and are therefore contaminated by valence quark contributions. An extraction of the low- x part of the transverse momentum distribution is in progress [16]. Note that the differential cross section increases at large transverse momentum faster with energy than at low q_\perp . The reason for this behavior is that at large q_\perp small dipole sizes are

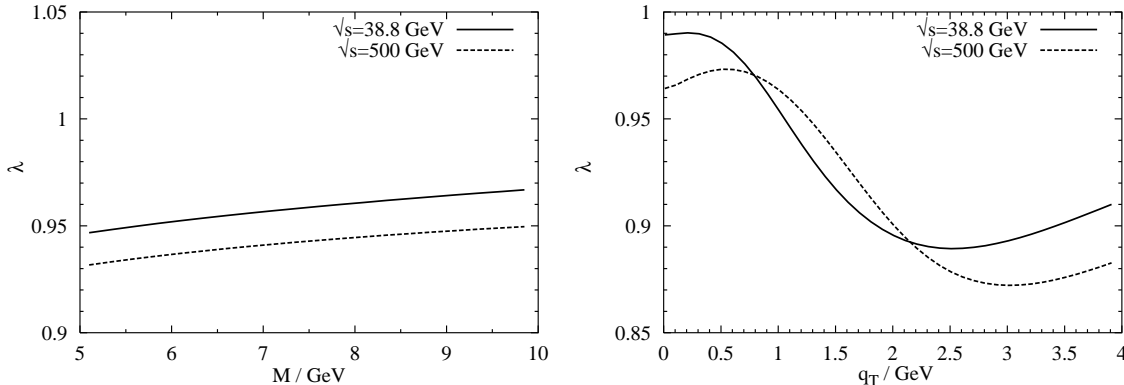


Figure 4: The left figure shows the dependence of the parameter λ , which describes the angular distribution of DY pairs (10) on the dilepton mass. The calculation is performed for $x_F = 0.625$. The figure on the right displays the q_\perp dependence of λ at $x_F = 0.625$ and $M = 6.5 \text{ GeV}$.

predominantly sampled, where the dipole cross section increases more rapidly with energy than at large separations. These large separations become more important at low q_\perp . The resulting broadening of transverse momenta with energy should not be confused with the well known broadening at fixed $\tau = M^2/s$, which can be understood from purely dimensional arguments.

The color dipole approach allows one to calculate separately the cross section for longitudinal and transverse photons. Experimentally, different polarizations can be distinguished by investigating the angular distribution of DY pairs, which can be written as

$$\frac{d\sigma}{dx_F dM^2 d\cos\theta} \propto 1 + \lambda \cos^2 \theta, \quad (10)$$

where θ is the angle between muon and the z -axis in the rest frame of the virtual photon. The parameter λ equals to ± 1 for transverse and longitudinal photons respectively. Therefore, it can be calculated as

$$\lambda = \frac{\sigma_T - \sigma_L}{\sigma_T + \sigma_L}. \quad (11)$$

Data for the angular distribution of DY pairs is usually presented in the dilepton center of mass frame and the value of λ depends on the choice of z -direction. Since the dipole approach is formulated in the target rest frame, it is convenient to put the z -axis in direction of the radiated photon [2]. The target rest frame and the dilepton center of mass frame are then related by a boost in z -direction. Note that in the dilepton center of mass frame, the z -axis is antiparallel to the target momentum. This frame is called the u -channel frame and the curves we present for λ are valid for this frame.

We study the dependence of λ on the dilepton mass and on the transverse momentum of the pair. Our results are shown in fig. 4. The deviation of λ from unity decreases very slowly with increasing mass. Although in fig. 4 (left) λ is slightly smaller at RHIC energies than at E772 energies, the deviation from a $1 + \cos^2 \theta$ distribution is typically a

5% effect. Note that in DY from pion-tungsten scattering at large x_F a sudden change of the angular distribution from $1 + \cos^2 \theta$ to $\sin^2 \theta$ has been observed [17]. This is usually explained by interactions of the spectator quark [18]. Such mechanisms are not included in the dipole approach. The K_1 -part in the transverse light cone wavefunction always dominates over the K_0 part in the longitudinal wavefunction. Thus, deviations from the $1 + \cos^2 \theta$ shape are always small.

As function of the transverse momentum q_\perp , fig. 4 (right), deviations from unity can become $\sim 10\%$ and λ exhibits an interesting nonmonotonous behavior which can be checked in future experiments. Note that in the parton model, the Lam-Tung relation [19] and helicity conservation require that $\lambda(q_\perp = 0) = 1$, which is obviously not the case in the dipole approach. Thus, the Lam-Tung relation is violated in the dipole approach. The reason for this behavior is caused by nonperturbative effects, which are parameterized in the dipole cross section. Using a parameterization $\propto \rho^2$ instead of (8) would yield $\lambda(q_\perp = 0) = 1$, as can be seen from eq. (16) in [3]. Experimentally, the Lam-Tung relation is found to be violated [17, 20].

We did not calculate the ϕ dependence of the cross section, since there is no hope that this will be measured within a foreseeable future. The only way to check the Lam-Tung relation in the not too far future is to study the limit $\lambda(q_\perp \rightarrow 0)$, which is possible at RHIC. It is a special virtue of the dipole approach, that one can easily perform calculations at $q_\perp \ll M$.

4 Summary

In this paper, the first realistic calculations in the color dipole approach to the DY process in proton-proton collisions are presented. We employ the parameterization [4] of the dipole cross section and find good agreement with E772 data [15] at low x_2 , without any K -factor or free parameter. The quark mass, which is in principle undetermined, has virtually no influence on the numerical results. The cross section steeply rises with energy and is about four times larger at RHIC than at Fermilab.

We also study the transverse momentum distribution of DY pairs. As a consequence of the saturation of the dipole cross section at large separations, the differential cross section does not diverge at zero transverse momentum, in contrast to the first order perturbative QCD correction to the parton model. The differential cross section rises with energy faster at large than at small momentum transfer. This correlates with the fact that the dipole cross section rises with energy steeper at small than at large separations.

We parameterize the angular distribution of the DY pairs as $(1 + \lambda \cos^2 \theta)$ and calculate the coefficient λ in the u -channel frame as a function of dilepton mass and transverse momentum. We find that λ as a function of M is typically around ~ 0.95 . In addition we find that λ does not go to unity for vanishing transverse momentum. This is a consequence of the parameterization of the dipole cross section which we employ. The behavior of λ at small q_\perp can be checked in proton-proton collisions at RHIC and possibly could point out the presence of dynamics beyond the QCD improved parton model.

Acknowledgments: This work was partially supported by the Gesellschaft für Schwerionenforschung, GSI, grant HD HÜF T, by the European Network *Hadronic Physics with Electromagnetic Probes*, Contract No. FMRX-CT96-0008, by the Graduiertenkolleg *Physikalische Systeme mit vielen Freiheitsgraden* and by the U.S. Department of Energy at Los Alamos National Laboratory under Contract No. W-7405-ENG-38. Part of this work was done, while J.R. was employee of the Institut für Theoretische Physik der Universität Heidelberg.

We are grateful to Jörg Hüfner and Mikkel Johnson for valuable discussions.

References

- [1] B. Z. Kopeliovich, proc. of the workshop Hirschegg '95: Dynamical Properties of Hadrons in Nuclear Matter, Hirschegg January 16-21, 1995, ed. by H. Feldmeyer and W. Nörenberg, Darmstadt, 1995, p. 102 (hep-ph/9609385).
- [2] S. J. Brodsky, A. Hebecker, and E. Quack, Phys. Rev. **D55** (1997) 2584.
- [3] B. Z. Kopeliovich, A. Schäfer, and A. V. Tarasov, Phys. Rev. **C59** (1999) 1609, extended version in hep-ph/9808378.
- [4] K. Golec-Biernat and M. Wüsthoff, Phys. Rev. **D59** (1999) 014017; Phys. Rev. **D60** (1999) 114023.
- [5] N. N. Nikolaev and B. G. Zakharov, Phys. Lett. **332B** (1994) 184; N. N. Nikolaev and B. G. Zakharov, JETP **78** (1984) 598.
- [6] A. B. Zamolodchikov, B. Z. Kopeliovich, and L. I. Lapidus, Sov. Phys. JETP Lett. **33** (1981) 612.
- [7] G. Bertsch, S. J. Brodsky, A. S. Goldhaber, and J. F. Gunion, Phys. Rev. Lett. **47** (1981) 297.
- [8] S. J. Brodsky and A. H. Mueller, Phys. Lett. **206B** (1988) 685.
- [9] J. D. Sullivan, Phys. Rev. **D5** (1972) 1732.
- [10] J. C. Peng et al. [E866/NuSea Collaboration], Phys. Rev. **D58** (1998) 092004.
- [11] M. B. Johnson, B. Z. Kopeliovich, J. Raufeisen, and A. V. Tarasov, paper in preparation.
- [12] J. Raufeisen, Ph.D. thesis Heidelberg 2000, hep-ph/0009358.
- [13] A. Milsztajn, A. Staude, K. M. Teichert, M. Virchaux, and R. Voss, Z. Phys. **C49** (1991) 527.
- [14] B. Z. Kopeliovich, A. Schäfer and A. V. Tarasov, Phys. Rev. **D62** (2000) 054022

- [15] E772 collab., P. L. McGaughey et al., Phys. Rev. **D50** (1994) 3038; erratum ibid. Phys. Rev. **D60** (1999) 119903.
- [16] J. M. Moss and M. J. Leitch, private communication.
- [17] J. S. Conway et al., Phys. Rev. **D39** (1989) 92.
- [18] E. L. Berger and S. J. Brodsky, Phys. Rev. Lett. **42** (1979) 940; E. L. Berger, Z. Phys. **C4** (1980) 289.
- [19] C. S. Lam and W. K. Tung, Phys. Rev. **D18** (1978) 2447; C. S. Lam and W. K. Tung, Phys. Rev. **D21** (1980) 2712.
- [20] NA10 collab., S. Falciano et al., Z. Phys. **C31** (1986) 513.